Global J. Environ. Sci. Manage. 5(1): 95-106, Winter 2019

Global Journal of Environmental Science and Management
(GJESM)

Homepage: https://www.gjesm.net/

ORIGINAL RESEARCH PAPER

Effect of digital elevation model's resolution in producing flood hazard maps

J.L. Ogania*, G.R. Puno, M.B.T. Alivio, J.M.G. Taylaran

Geo-Safer Project, College of Forestry and Environmental Science, Central Mindanao University, Musuan, Bukidnon, Philippines

ARTICLE INFO

Article History:
Received 26 August 2018
Revised 30 October 2018
Accepted 7 November 2018

Keywords:
Disaster
Geographic information system (GIS)
Hydrologic engineering centre-hydrologic modeling system (HEC-HMS)
Inundation
River analysis system (RAS)

ABSTRACT

Flooding is one of the most devastating natural disasters occurring annually in the Philippines. A call for a solution for this malady is very challenging as well as crucial to be addressed. Mapping flood hazard is an effective tool in determining the extent and depth of floods associated with hazard level in specified areas that need to be prioritized during flood occurrences. Precedent to the production of maps is the utilization of reliable and accurate topographic data. In the present study, the performance of 3 digital elevation models having different resolution was evaluated with the aid of flood modeling software such as hydrologic engineering centre-hydrologic modeling system and hydrologic engineering centre-river analysis system. The two-dimensional models were processed using three different digital elevation models, captured through light detection and ranging, interferometric synthetic aperture radar, and synthetic aperture radar technologies, to simulate and compare the flood inundation of 5-, 25- 100-year return periods. The accuracy of the generated flood maps was carried out using statistical analysis tools - Overall accuracy, F-measure and root-mean-square-error. Results reveal that using light detection and ranging–digital elevation model, the overall accuracy of the flood map is 82.5% with a fitness of 0.5333 to ground-truth data and an error of 0.32 meter in simulating flood depth which implies a promising performance of the model compared to other data sources. Thus, higher resolution digital elevation model generates more accurate flood hazard maps while coarser resolution over-predicts the flood extent.

DOI: 10.22034/gjesm.2019.01.08

INTRODUCTION

The Philippines is one of the countries primarily affected by flooding caused by typhoon due to its archipelagic and geographic location (Ginnette, 2013; Senate Economic Planning Office, 2013; Calang, 2017). It ranked as 3rd next to China and India that has been reported with natural disasters' incidence (Juban *et al.*, 2012). Typhoons usually occurred every year (y) and some left the country with casualties and/or damages (ADRC, 2013; Dela Cruz, 2016). The impact repeats as typhoon visit the country because disasters preparedness is not yet fully implemented due to the absence of baseline information and collaborative effort in eradicating those impacts. Flood modeling has become a typical method in simulating flood scenarios and inundation maps for effective identification of areas to be monitored

*Corresponding Author:
Email: *jeniferogania@gmail.com*
Tel.: +639107 446317
Fax: +63 (88) 356 1912

Note: Discussion period for this manuscript open until April 1, 2019 on GJESM website at the "Show Article.

when flooding is going to occur. Through the use of flood modeling software - HEC-HMS and HEC-RAS, the simulations of hydrologic and hydraulic data were done to calibrate basin model (Puno and Barro, 2016) and to produce flood hazard maps (Puno *et al.,* 2018), respectively. However, the result of this simulation greatly depends on the availability of accurate topographic data that can represent the ground-truth of modeled area to produce a near-real-time flood scenario as possible (Podhorányi *et al.,* 2013). Digital elevation model (DEM) as the primary baseline of ground topography has a significant influence on the calculated river hydraulics and the extent of inundation areas (Nicholas and Walling, 1997; Horritt and Bates, 2001) and it is therefore important that its resolution be optimized to the greatest possible extent (Casas *et al.* 2006). Saksena (2015) confirmed that the resolution of DEM plays an important role in the reliability of the generated flood hazard map. In recent years, Philippine research studies are using the DEM out of light detection and ranging (LiDAR), Interferometric Synthetic Aperture Radar (IFSAR), and Synthetic Aperture Radar (SAR) technologies. These were considered because of its higher resolution compared to the other DEM offered online. LiDAR is a remote sensing technology that uses laser pulse in measuring variable distances to the Earth and it generates actual, three-dimensional information of the configuration of the Earth and its surface characteristics (NOAA, 2012; UPD-TCAGP, 2013). LiDAR-derived data are well-known and attractive due to its high horizontal resolution (USGS, 2008; Dowman, 2014; Chen *et al.,* 2017) and vertical accuracy (Gillin *et al.,* 2015; Chen *et al.,* 2017) and became a most useful tool in hydrodynamic modeling and flood mapping (Wedajo, 2017). The elevation data from LiDAR is used to provide inputs such as river cross-section geometry, floodplain topography (Council, 2007, 2009), and flood-plain roughness (Mason *et al*., 2003; Casas *et al*., 2010) for flood inundation models. However, acquiring such data is costly (Hummel *et al.,* 2011) thus it limits and prioritizes the acquisition in highly vulnerable areas to flooding. Other alternatives such as IFSAR and SAR DEM were also used in the absence of LiDAR with a larger area covered. IFSAR and SAR DEMs were gathered using transmitted pulses of radio waves to illuminate a target scene and echo of each pulse is received and recorded that allows the creation of higher-resolution images (Mercer, 2001). Several countries were still using and relying on coarser resolution, less accurate DEMs to create flood inundation maps (Sanders, 2007). Further, the advocate on the use of high-resolution DEMs is increasingly catching much attention in flood modeling studies (Haile and Rientjes, 2005). Numerous studies have been directed on the importance of higher resolution DEMs in flood inundation mapping which produces more accurate flood maps (Brandt, 2005; Marks and Bates, 2000; Omer *et al*., 2003; Werner, 2001; Puno and Amper, 2016; Puno *et al.*, 2016). In the Philippines, DEMs of LiDAR, IFSAR, and SAR were currently being used in flood modeling studies having a 1 and 5-meters, and 10-meter (m) resolution, respectively. However, the outputs of these 3 DEMs were significantly different due to its various resolutions. Particularly, the most reliable inundation maps are generated with the use of more detailed and 1 m resolution DEM produced by LiDAR technology (Haile and Rientjes, 2005). LiDAR data has a horizontal resolution of as high as 0.5 m and vertical accuracy of 0.15 to 0.25 m (Aguilar *et al.*, 2010; Giglierano, 2010 and Smith, 2010) which is deemed advantageous in producing accurate flood maps compared to other DEMs. The resolution and accuracy of DEM influences and have a substantial impact on water surface elevations and flood extents (Saksena, 2015). Consequently, flood modeling best performs in LiDAR DEM compared to other DEM data sources (Hailes and Rientjes, 2005 and Schumann *et al*., 2008). Thus, this study will present the outputs of three different DEMs to illustrate and suggest the applicability of using LiDAR-derived DEM in flood inundation mapping and its comparison with SAR and IFSAR DEMs in generating flood hazard maps are not yet elucidated which leaves a wide gap in the field of research. Correspondingly, this has become the subject for research towards higher resolution and accurate flood hazard maps for disaster preparedness and risk mitigation. This study has been carried out in Taganibong Watershed, situated in the province of Bukidnon, Mindanao, Philippines in 2018 under the project of geo-informatics for the systematic assessment of flood effects and risks (GeoSAFER) for a resilient northern Mindanao/ Cotabato of Central Mindanao University (CMU). This project is the continuation of the project entitled Philippine-LiDAR 1 (Phil-LiDAR 1) headed by University of the Philippines – Diliman (UPD) which it aims to develop

flood hazard maps of all the critical river in the nation.

MATERIALS AND METHODS

Location of the Study

Taganibong Watershed is located in the province of Bukidnon, southeast of Cagayan de Oro City in the island of Mindanao, Philippines with a geographical coordinates of 7° 48' 46.7" north to 7° 56' 11.84" north latitudes and 124° 56' 59.36" east to 125° 4' 41.56" east longitudes. The watershed is elongated in shape (Puno *et al.,* 2015) and has an estimated area of 6,000 hectares (ha). It has an approximate lowest elevation of 277 m and highest elevation of 1,334 m. Taganibong river traverses from its headwaters in Valencia City and drains to Pulangi River for an about 30 kilometers (km). The river has caused flooding (Puno *et.al.,* 2015) specifically in the area of CMU and it contributes to the water level rise of Pulangi River, one of the major rivers in the province of Bukidnon (Galarpe *et al.,* 2017) and one of the major tributaries of Rio Grande de Mindanao (Pradhan *et al.,* 2016; UPLB, 2017).

DEM processing

Due to its various resolution, IFSAR and SAR DEMs were resampled into 1-meter using the raster calculator tool in ArcGIS 10.2 to make it similar and comparable with LiDAR DEM. Bathymetric data consists of the riverbed elevation was interpolated using the Inverse Distance Weighted (IDW), an interpolation tool in ArcGIS 10.2, which it uses a linearly weighted combination of a set of bathymetric data points to determine cell values and to create its own DEM. The resulted bathymetric DEM was integrated into each DEM using the feathering tool developed by UPD. Hillshade tool was then used in presenting the terrain of each DEM. Moreover, the 10-m contour lines and percent slope classes were also generated by processing the DEM using ArcGIS 10.2 spatial analyst tool to show the spatial difference of the 3 DEMs. By examining these parameters it would define how detailed and high resolution the DEMs and could support the differences in further results.

Basin model pre-processing

Taganibong River channel and a 10 m resolution SAR-DEM were the primary data used in creating a basin model. The river channel was digitized using Google Earth while SAR-DEM was gathered from UPD during the implementation of Phil-LiDAR 1 project last 2014-2017. SAR-DEM was considered since it covers the whole stretch of the basin. The data were processed using GeoHMS10.2 tool plugin in ArcGIS 10.2 to generate an HMS basin model and

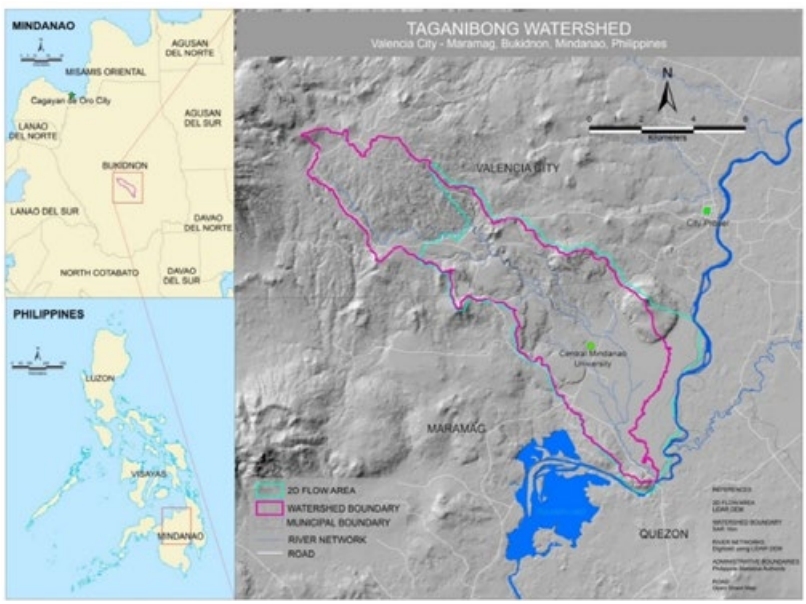


Fig. 1: Geographical location of Taganibong Watershed in the Philippines

incorporated with the available soil and land cover data of 2004 from National Mapping and Resource Information Authority (NAMRIA) to assign curve number (CN) in each sub-basin. CN will represent the soil type and land cover classification of each sub-basin. Other parameters such as initial abstraction (IA), time of concentration (TC), Storage Coefficient (SC), River Length and sub-watershed area were also derived during the pre-processing of basin model. These parameters were extracted to be used for further basin model calibration in which it helps in moving and forming the simulated hydrograph.

HMS basin model calibration and RIDF simulations

Utilizing the hydrological and surveyed data gathered from the field (UPD-TCAGP, 2013), the HMS Basin Model, the output of pre-processing, was calibrated under the HEC-HMS 3.5 standalone software, to simulate the hydrologic response of the watershed to a given hydrometeorological input (Zhang *et al.,* 2013). Water Level, velocity and river cross-section data were used in calculating the river discharge tied in mean sea level (MSL). The calculated actual river discharge with a higher value of R-squared and simultaneous rainfall data are the primary data requirement in proceeding to HMS model calibration (Scharffenberg and Fleming, 2010). In calibrating the model, parameters were used for the following methods: CN and IA for Loss – Soil Conservation Service (SCS) CN method; TC and SC for Transform – Clark Unit Hydrograph method; Initial Discharge (ID), Recession Constant (RC) and Ratio to Peak (RP) for Baseflow – Recession method and; length, slope, Manning's N and width for Routing – Muskingum-Cunge method. Based on physical observation during model calibration, values of CN and IA are manually adjusted to increase or decrease the magnitude and SC and TC to move left or right the simulated hydrograph. Besides, the parameters' values of Baseflow – Recession method is used to fit with the initial flow and recession while parameters of Routing – Muskingum-Cunge method is adjusted to smoothen or coarsen the simulated hydrograph. Calibration is necessary to make the simulated hydrograph similar or close to the actual hydrograph (Krause *et al.,* 2005). Parameters' values were adjusted several times to achieve an at least satisfactory performance rating in all the statistical measures recommended for model evaluation. This is relevant to assess the accuracy of the calibrated model. The accuracy tests such as Nash-Sutcliffe Efficiency (NSE), Percent Bias (PBias), and the ratio of the root mean error to the standard deviation of measured data (RSR) were used in evaluating the model. The model is assessed as calibrated if NSE>0.5, if PBIAS$\pm$25%, and if RSR$\leq$0.70 (Moriasi *et al.,* 2007). As the model is calibrated, the simulations of rainfall scenarios of 5-, 25, 100-y follows. The Rainfall Intensity Duration Frequency (RIDF) data for the above-mentioned return periods was acquired from Philippine Atmospheric, Geophysical and Astronomical Services Administration (PAGASA) Malaybalay rain gauge station with 31-y rainfall records. These data were inputted as the meteorological model file using frequency storm precipitation method in HEC-HMS performed with calibrated basin model. The outputs of the simulations were the calibrated basin model with precipitation and outflow data of the 3 return periods.

Two-dimensional (2D) RAS model simulations

The 3 processed DEMs were separately utilized in processing the River analysis system (RAS) model under the HEC-RAS 5.0 software, hydraulic modeling software useful in rainfall-run-off simulations (USACE, 2010) and to determine flood-prone areas (Santos and Tavares, 2012). The 2D flow area with an area of 5305.36 ha, as primary data requirement in the RAS geometric data, was created using GeoRAS extension tool in ArcGIS 10.2 considering the extent of the floodplain of the watershed. Fig. 2 shows the resulted geometric data used in flood inundation simulations. The RAS model was processed through unsteady flow analysis and boundary condition data for RAS model simulations was set. The boundary condition data such as calibrated HMS outflow and precipitation of 5-, 25-, and 100-y were integrated into the model through inflow point and 0.01 was assumed as a normal depth of the 2D Model. Breaklines such as road networks and bridges were also integrated to define areas with a change in elevation.

Flood hazard mapping and accuracy assessment

In mapping the flood hazard, the generated flood depths from 2D RAS model simulations were extracted and map-out in ArcGIS 10.2 and categorized into Low (0-0.5m), Medium (>0.5m – <1.5m), and High (>1.5m) according to Department of Science and Technology's

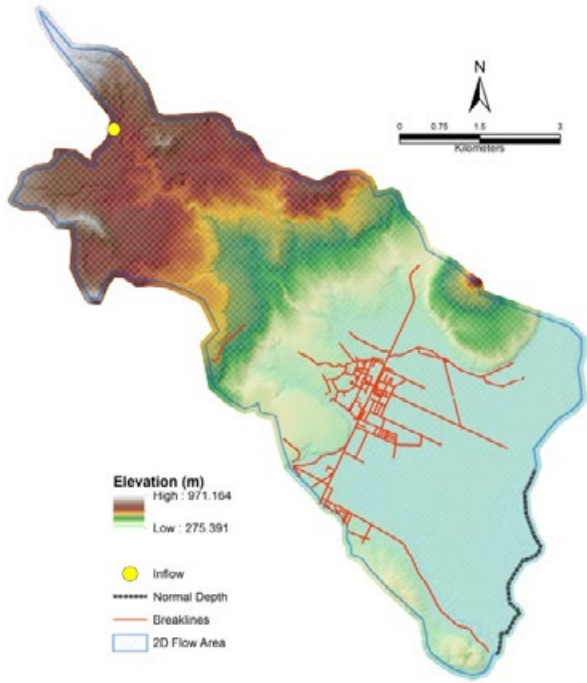


Fig. 2: Taganibong Hydrologic modeling system,
River analysis system geometric data using LiDAR DEM

(DOST's) flood hazard level standard overlaid with the 2D flow area and the DEM used in the simulation. Moreover, the accuracy assessment of flood hazard maps was conducted using flood validation points of Typhoon Pablo in 2013. Flood validation points were gathered using a handheld global positioning system (GPS) and actual flood depth was recorded in a given field data sheet. Using ArcGIS 10.2, the flood validation points were converted into shape files and actual flood depth information was encoded into its attribute table. Typhoon Pablo rainfall data was utilized as a source of meteorological input through inverse distance precipitation method simulated with calibrated basin model under HEC-HMS 3.5. The simulation provides precipitation and outflow data and was used as boundary condition data in unsteady flow analysis of HEC-RAS 5.0. Then the flood depths of Typhoon Pablo were generated using each DEM. Each flood depth was added in ArcGIS 10.2 together with the flood validation points. Using raster calculator and extract values to point's tool, the simulated flood depth values correspond to each flood validation points were extracted. The root mean square error (RMSE) (Chai and Draxler, 2014), F-measure (Hripcsak and Rothchild, 2005) and overall accuracy were then computed to assess the model performance and prediction. The model is assessed as good if RMSE is closer to 0, F-measure<0.5, and overall accuracy<70%.

RESULTS AND DISCUSSION

Processed DEM

Most studies in the past have shown the importance of DEM resolution in flood inundation mapping and concluded that DEM with higher resolution produces more accurate flood maps compared to coarser resolution DEM which over-predict the flood extents (Brandt, 2005; Cook and Merwade, 2009; Werner, 2001). DEM represents topography (Weepener *et al.*, 2012) of the river and floodplain as an important aspect of hydraulic flood modeling, the accuracy of which influence estimates of flood damage. Thus, in this study, elevation is resampled and the contour lines and percent slope were calculated to compare the flood inundation provided by using different DEM. The difference of elevation, contour lines and slope of each DEM were shown in Figs. 3, 4, and 5, respectively. It entails then that major flooding may

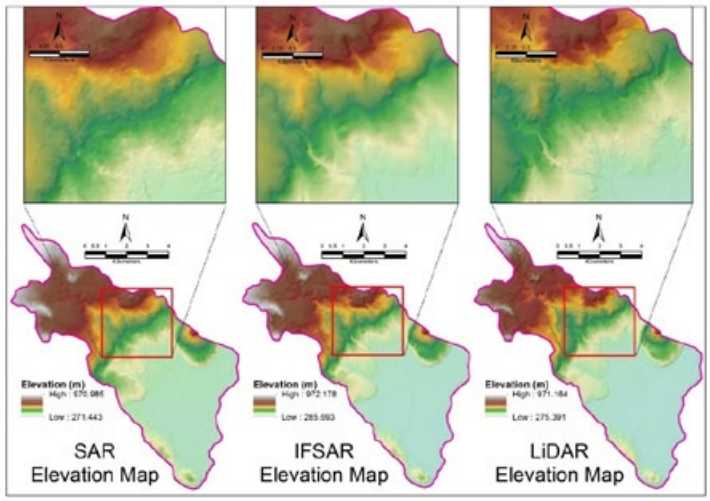


Fig. 3: Digital elevation model used in simulating flood inundation

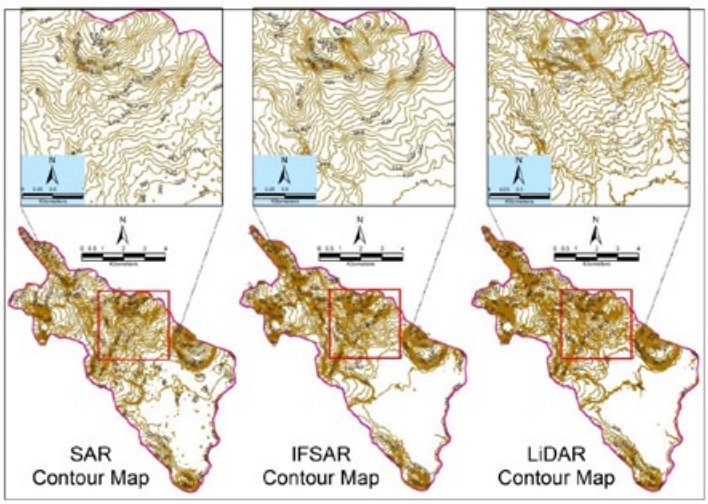


Fig. 4: Comparison of contour lines

occur in downstream location since flood water will flow to where the elevation is low (Mina *et al.,* 2015). In consequence, a more pronounced effect of greater risk of casualties and damages to infrastructure and establishments is expected downstream. Getahun and Gebre (2015) use elevation and slope as one of the flood generating factors for flood hazard assessment and mapping. On the other hand, the importance of slope in flood inundation determines how quickly a drainage channel will convey water, thus, it influences the sensitivity of a watershed to precipitation events of various time durations. The lower the slope value is the flatter the terrain and in the same way the higher the slope value is the steeper the terrain (Brewer and Marlow, 1993; Tang and Pilesjo, 2011). Steep slopes tend to result in rapid runoff responses to local rainfall excess and consequently higher peak discharges since rain is less likely to infiltrate into the ground. This caused the river to burst its bank with more overland flow and a quicker overland flow rate (Tom, 2018). Flat slope responding to the same rainfall amount will not be as rapid and the frequency of the resulting discharge maybe dissimilar to the storm frequency since gentle slopes allow water to penetrate into the soil and increase lag times (McCuen *et al.,* 2002). In addition,

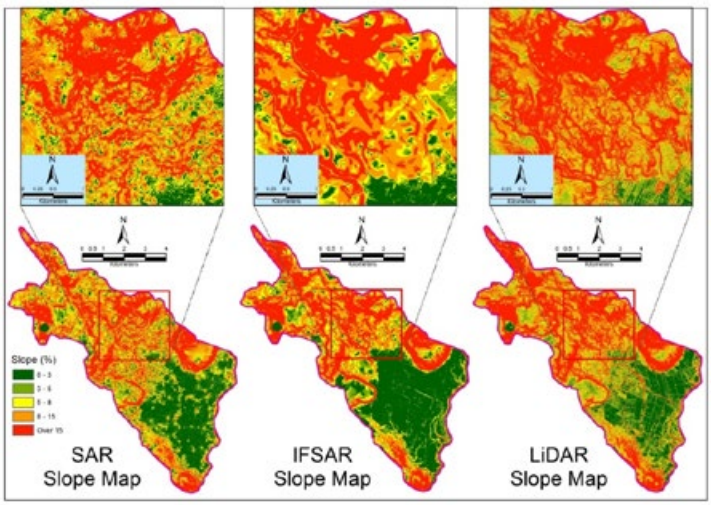


Fig. 5: Comparison of percent slope

elevation and slope can be described through examining contour lines. The closer the contour lines, the steeper its slope and the wide-spaced contour lines signify a gentle slope. Results of the contour lines and slope in each DEM differ in its distribution spacing, and level, respectively, thus considering DEM in simulating flood inundation plays an essential role in determining its reliability.

Basin model

As shown in Fig. 6, Taganibong basin model has 31 sub-basins, 20 reaches, and 18 junctions. It was calibrated using the 18-hour rainfall event last December 31, 2017- January 1, 2018. The calibrated basin model got a very good performance rating based on the model evaluation using NSE for model trends, RSR for its residual variation and PBIAS for its average magnitude with a value of 0.77, 0.48 and -5.30, respectively. These statistical measures were used in determining the efficiency of the model and it illustrates a well-calibrated model in which the model's observed and simulated discharge data were closely fitted to each other with an R^2 of 0.79.

Flood hazard maps and accuracy assessment

The flood hazard maps using rainfall scenarios give the probability of flood occurrence in the area within a y and it provides information that may help the community able to prepare for the possible situation. The flood hazard maps of 5-, 25-, 100-y predict the possible flood inundation when accumulated rainfall

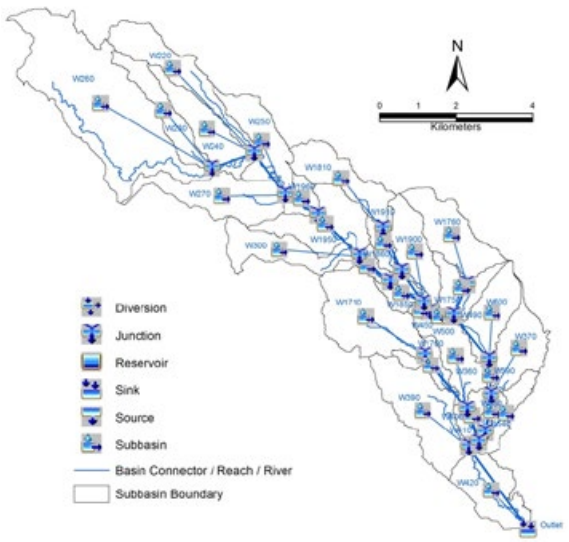


Fig. 6: Taganibong hydrologic modeling system model

amount of 153.6 mm, 214.8 mm and 265.3 mm will occur within 24 hours, respectively. Using the 3 return periods the objective of the study was supported in which results compare the capacity of predicting flood occurrences and define the difference of inundation area and hazard levels of the 3 DEMs. The resulted flood hazard maps revealed the difference of the outputs in which resolution really affects the inundation and its hazard levels as the return period varies. As shown in Figs. 7, 8 and 9 the maps using LiDAR-DEM produced a define flood extent and

shows clearly the distribution of hazard levels inside the 2D flow area or in the assigned floodplain. Table 1 shows the total flooded area per return period per DEM. It stated that maps out of LiDAR-DEM produced define area with 30.51 %, 35.47% and 42.24% of the total area of the assigned floodplain for the rainfall scenarios of 5-, 25- 100-y, respectively, and it shows that there are different result in all of the simulations based on the flood hazard levels and flood inundations.

The accuracy of each flood hazard maps generated from 3 different DEM data sources was assessed using a confusion matrix approach. It is used to show the accuracy of the generated flood maps by comparing the records of the modeled flood from the actual flood data. Overall accuracy or the classification accuracy indicates the proportion of the correctly predicted points over the total collected data (Jung *et al.,* 2014) which implies how a flood hazard could be mapped at a certain level of accuracy. F-measure is the measure of fitness or the goodness of fit between the created flood map and ground-truth data (Gall *et al.,* 2007) while the RMSE sums up the differences of two values (Ternate *et al.,* 2017). As depicted in Table 2 confirms the result of the accuracy assessment that flood map driven by LiDAR-DEM data and showing a promising

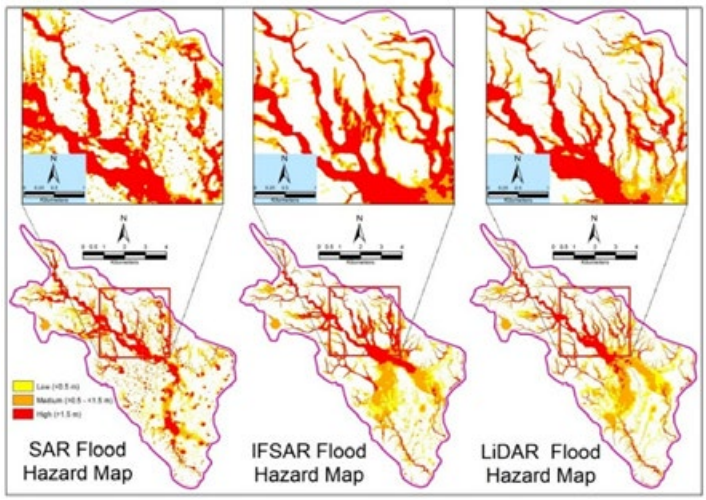


Fig. 7: RAS simulation results using RIDF 5-year

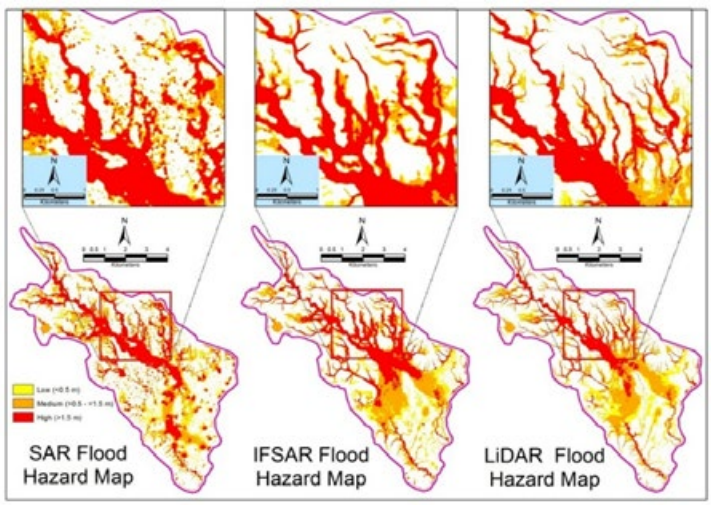


Fig. 8: RAS simulation results using RIDF 25-year

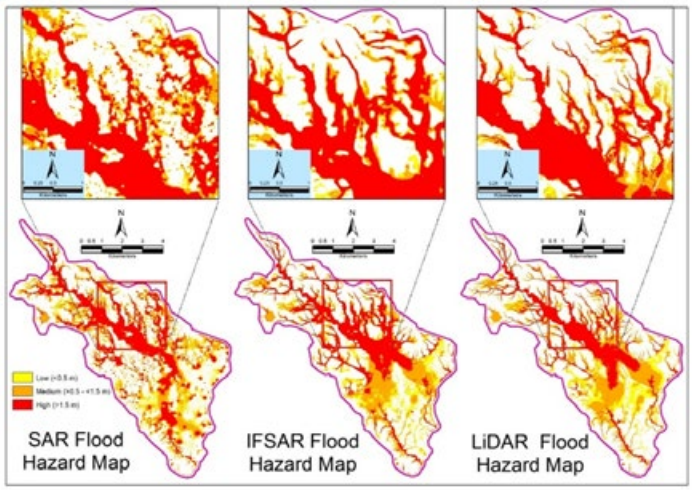


Fig. 9: RAS simulation results using RIDF 100 year

Table 1: Flood inundation results

Return period	SAR (ha)	IFSAR (ha)	LiDAR (ha)
5-y	1623.1	1733.5	1618.7
25-y	2176.4	2176.8	1882.1
100-y	2474.1	2421.2	2241.1

Table 2: Flood map accuracy assessment of three DEM data sources

DEM data source	Overall accuracy	F-measure	RMSE (m)
LiDAR	82.5%	0.5333	0.32
IFSAR	73.33%	0.4286	0.88
SAR	65.83%	0.2807	1.12

performance that out of the collected points from the field, 82.5% of which is correctly classified as flooded by the model with an acceptable value of F-measure. The calculated RMSE indicates that the model can simulate flood depths with an error that can reach 0.32 m. On the other hand, flood map generated from SAR DEM with coarser resolution has the lowest overall accuracy and F-measure with the highest error in simulating flood depths. Incongruent to the generated flood inundation area of each DEM data source as presented Table 1, coarser resolution DEM over-predict the generated flood extents which are in agreement to the result of (Brandt, 2005; Cook and Merwade, 2009; Werner, 2001) that DEM with higher resolution produces more accurate flood maps. It can be deduced then for this study, higher overall accuracy and F-measure with smaller RMSE value yields to more accurate flood hazard maps. Nevertheless, IFSAR DEM could be an alternative in the absence of LiDAR DEM considering the cost of acquiring LiDAR derivative data.

CONCLUSION AND RECOMMENDATION

DEM resolution plays a significant role in generating flood inundation maps in which it represents the topographic data of the river and the floodplain. Moreover, higher resolution DEM provides more accurate and reliable maps in the field of flood simulations. LiDAR-derived flood hazard maps provide more define flood extent and clearly show the distribution of hazard levels. Among the other, it is better and accurate in predicting flood inundation. Through the use of these maps, it will help the disaster risk reduction and management (DRRM) team in identifying specific areas need to be

monitored and prioritized for DRRM operation when such return period occurs. As well as it can provide an initial assessment of the possible population and areas that could be affected by low, medium, and high hazard. Moreover, it specifies not flooded areas that can be potential for the establishments of evacuation centre or a venue for other infrastructural development. Thus, it is highly recommended that the local government units (LGUs) must consider the use of more detailed and accurate data as LiDAR-DEM in generating flood maps as the best tool for disaster preparedness and prevention as well. However, it is still necessary to conduct flood validation before the full implementation and usage of flood inundation maps.

ACKNOWLEDGMENT

This study is a product of the project entitled "Project 2 - GeoSAFER Northern Mindanao/ Cotabato: Systematic assessment of flood effects and risks in Northern Mindanao and Cotabato, Philippines" supported by the Philippine Council for Industry, Energy and Emerging Technology Research and Development (PCIEERD), Department of Science and Technology (DOST). The authors are also grateful to CMU administration for its support.

CONFLICT OF INTEREST

The authors declare that there are no conflicts of interest regarding the publication of this manuscript. In addition, the ethical issues; including plagiarism, informed consent, misconduct, data fabrication and/or falsification, double publication and/or submission, redundancy has been completely observed by the authors.

ABBREVIATIONS

2D	Two-dimensional
ARG	Automated rain gauge
CMU	Central Mindanao University
CN	Curve number
DEM/s	Digital elevation model (s)
DOST	Department of Science and Technology
DRRM	Disaster risk reduction and management
GIS	Geographical information system
GPS	Global positioning system
GeoSAFER	Geo-informatics for the systematic assessment of flood effects and risks
ha	Hectare
HEC-HMS	Hydrologic Engineering Centre - Hydrologic modeling system
HEC-RAS	Hydrologic Engineering Centre - River analysis system
km	Kilometre
IA	Initial Abstraction
ID	Initial discharge
IDW	Inverse distance weighed
IFSAR	Interferometric synthetic aperture radar
LGU	Local government unit
LiDAR	Light detection and ranging
m	Meter
MSL	Mean sea level
NAMRIA	National mapping and resource information authority
NSE	Nash-Sutcliffe Efficiency
PAGASA	Philippine Atmospheric, Geophysical, and Astronomical Services Administration
PBias	Percent bias
PCIEERD	Philippine Council for Industry, Energy and Emerging Technology Research and Development
RC	Recession constant
RIDF	Rainfall intensity duration frequency
RMSE	Root mean square error
RP	Ratio to peak
RSR	Ratio of the root mean error to the standard deviation
SAR	Synthetic aperture radar
SC	Storage coefficient
SCS	Soil conservation service
TC	Time of concentration

REFERENCES

ADRC, (2013). Information on disaster risk reduction of the member countries. Asian Disaster Reduction Centre.

Aguilar, F.J.; Mills, J.P.; Delgado, J.; Aguilar, M.A.; Negreiros, J.G.; Pérez, J.L., (2010). Modeling vertical error in LiDAR-derived digital elevation models. ISPRS J. Photogram. Remote Sens., 65(1): 103–110 (8 pages).

Bates, P.D.; Marks, K.J.; Horritt, M.S., (2003). Optimal use of high-resolution topographic data in flood inundation models. Hydrol. Process., 17 (3): 537–557 (21 pages).

Brandt, S., (2005). Resolution issues of elevation data during inundation modeling of river floods. Proceedings of the XXXI IAHR Congress, 3573–3581 (9 pages).

Brewer, C.; Marlow, K., (1993). Color representation of aspect and

slope simultaneously. Eleventh International Symposium on Computer-Assisted Cartography (Auto-Carto-11), Minneapolis, Minnesota. October 1993.
Calang, M.G., (2017). The Philippine Disaster Risk Reduction and Management (DRRM) system. A country report compiled by ADRC.
Chai, T.; Draxler, R., (2014). Root mean square error (RMSE) or mean absolute error (MAE)? –
arguments against avoiding RMSE in the literature. Geosci. Model Dev., 7: 1247–1250 (4 pages).
Casas, A.; Benito, G.; Thorndycraft, V.R.; Rico, M., (2006). The topographic data source of digital terrain models as a key element in the accuracy of hydraulic flood modelling. Earth Surface Processes and Landforms, 31 (14): 444-456 (13 pages).
Casas, A.; Lane, S.N.; Yu, D.; Benito, G., (2010). A method for parameterising roughness and topographic sub-grid scale effects in hydraulic modelling from LiDAR data. Hydrol. Earth Syst. Sci., 14: 1567-1579 (13 pages).
Chen, B.; Krajewski, W. F.; Goska, R.; Young, N., (2017). Using LiDAR surveys to document floods: A case study of the 2008 Iowa flood. J. Hydrol., 553: 338–349 (12 pages).
Cook, A.; Merwade, V., (2009). Effect of topographic data, geometric configuration and modeling approach on flood inundation mapping. J. Hydrol., 377(1-2): 131–142 (12 pages).
Dela Cruz, G., (2016). In numbers: Typhoons in the Philippines and the 2016 polls.
Dowman, I., (2014). Integration of LiDAR and IFSAR for mapping. University College London. Invited paper Commission II, WGII/2.
Galarpe, V.R.K.; Heyasa, K.J.; Heyasa B.B., (2017). Water quality and risk assessment of tributary rivers in San Fernando, Bukidnon, Philippines. JBES, 1: 266-273 (8 pages).
Gall, M.; Boruff, B. J.; Cutter, S. L., (2007). Assessing flood hazard zones in the absence of digital floodplain maps: Comparison of alternative approaches. Nat. Hazards Rev., 8(1): 1–12 (12 pages).
Getahun, Y. S.; Gebre, S. L., (2015). Flood hazard assessment and mapping of flood inundation area of the Awash River Basin in Ethiopia using GIS and HEC-GeoRAS/HEC-RAS Model. J. Civil Environ. Eng., 5(4): 1-12 (12 pages).
Gillin, C.; Bailey, S.; McGuire, K.; Prisley, S., (2015). Evaluation of LiDAR-derived DEMs through terrain analysis and field comparison. PE&RS, 81(5): 387-396 (10 pages).
Giglierano, J.D., (2010). LiDAR basics for natural resource mapping applications. Geol. Soc., Lond., Special Publ. 345(1): 103–115 (12 pages).
Ginnette, J., (2013). Disaster-induced internal displacement in the Philippines. The case of Tropical Storm Washi/Sendong. A report of the Internal Displacement Monitoring Centre.
Haile, A.T.; Rientjes, T.H.M., (2005). Effects of LiDAR DEM resolution in flood modeling: a model sensitivity study for the city of Tegucigalpa, Honduras. ISPRS WG III/3, III/4, V/3 Workshop, Netherlands, September 12-14, 2005.
Hripcsak, G.; Rothchild, A., (2005). Agreement, the F-measure, and reliability in information retrieval. Technical Brief on agreement in information retrieval. 12: 296-298 (3 pages).
Horritt, M.S.; Bates, P.D., (2001). Effects of spatial resolution on a raster based model of flood flow. J. Hydrol., 253(1-4): 239-249 (11 pages).
Hummel, S.; Hudak, A.T.; Uebler, E.H.; Falkowski, M.J.; Megown, K.A., (2011). A comparison of accuracy and cost of LiDAR versus stand exam data for landscape management on the Malheur national forest. J. For., 267-273 (7 pages).
Juban, N.R.; Bermudez, A.N.C.; Sarmiento, R.F.R.; Dumagay, J.A.E., (2012). The epidemiology of disasters: Health effects of flood disasters in the Philippines. International Symposium on the impacts of increasing flood risk on food and health security in Southeast Asia, At Kyoto, Japan. March 2012.
Jung, Y.; Kim, D.; Kim, D.; Kim, M.; Lee, S., (2014). Simplified flood inundation mapping based on flood elevation-discharge rating curves using satellite images in gauged watersheds. Water, 6(5): 1280–1299 (20 pages).
Krause, P.; Boyle, D.P.; Base, F., (2005). Comparison of different efficiency criteria for hydrological model assessment. European Geosciences Union. Adv. Geosci., 5: 89–97 (9 pages).
Marks, K.; Bates, P., (2000). Integration of high-resolution topographic data with floodplain flow models. Hydrol. Process., 14 (11-12): 2109– 2122 (14 pages).
Mason, D.C.; Cobby, D.M.; Horritt, M.S.; Bates, P.D., (2003). Floodplain friction parameterization in two-dimensional river flood models using vegetation heights derived from airborne scanning laser altimetry. Hydrol. Process, 17 (9): 1711–1732 (22 pages).
McCuen, R.; Johnson, P.; Ragan, R., (2002). Highway hydrology. United States Department of Transportation, Federal Highway Administration–National Highway Institute, Hydraulic design series No. 2, second edition.
Mercer, B., (2001). Comparing LIDAR and IFSAR: What can you expect? Inter-map Technologies Corp. Proceedings of Photogrammetric Week 2001, Stuttgart, Fritsch/Spiller (Eds.).
Mina, A.; Michaels, G.; McDermott, T.; Rauch, F., (2015). Despite their exposure to flooding, low elevation urban areas concentrate a high density of economic activity. Centre Piece Winter.
Moriasi, D.N.; Arnold, J.G.; Van Liew, M.W.; Binger, R.L.; Harmel, R.D.; Veith, T.L., (2007). Model evaluation guidelines for systematic quantification of accuracy in watershed simulations. Trans. ASABE, 50(3): 885-900 (6 pages).
National Oceanic and Atmospheric Administration (NOAA) Coastal Services Center, (2012). LiDAR 101: An introduction to Lidar technology data and applications. Revised. Charleston, SC: NOAA Coastal Services Center.
National Research Council, (2007). Elevation Data for Floodplain Mapping. The National Academies Press.
National Research Council, (2009). Mapping the Zone: Improving Flood Map Accuracy. The National Academies Press.
Nicholas, A.P.; Walling, D.E., (1997). Modelling flood hydraulics and overbank deposition on river floodplains. Earth Surf. Process. Landf., 22(1): 59-77 (19 pages).
Omer, C.; Nelson, E.; Zundel, A., (2003). Impact of varied data resolution on hydraulic modeling and floodplain delineation. J. Am. Water Resour. Assoc. (JAWRA), 39(2): 467–475 (8 pages).
Puno, G.R.; Amper, R.A.L., (2016). Flood modeling of Musimusi river in Balingasag, Misamis Oriental. CMUJS, 20(3): 150-165 (16 pages).
Puno, G.; Amper, R.A.; Talisay, B.A., (2018). Flood simulation using geospatial and hydrologic models in Manupali watershed, Bukidnon, Philippines. J. Bio. Environ. Sci., 12(3): 294-303 (10 pages).
Puno, G.; Barro, R.A., (2016). Alubijid river basin hydrologic modeling in Misamis Oriental for flood risk management. CMUJS, 20(3): 97-106 (10 pages).
Puno, G.R.; Talisay, B.A.T.; Paquit, J.C., (2016). GIS-based flood hazard mapping in Gingoog river, Mindanao. CMUJS, 20(3): 81-96 (16 pages).
Puno, G.; Villar, R.; Bruno A.G.; Corpuz, O., (2015). GIS-based

mapping and morphometric analysis of flood prone sites in the three watersheds of Bukidnon. Int. J. Biotechnol. Allied Fields, 3(7): 121-129 (9 pages).

Pradhan, N.R.; Byrd, A.; Jourdan, M.; Ellis, J., (2016). Development of predictive relationships for flood hazard assessments in ungaged basins.

Podhorányi, M.; Unucka, J.; Bobál', P.; Říhová, V., (2013). Effects of LIDAR DEM resolution in hydrodynamic modelling: model sensitivity for cross-sections. IJDE, 6(1): 3–27 (25 pages).

Saksena, S., (2015). Investigating the role of DEM resolution and accuracy on flood inundation mapping. World Environmental and Water Congress. Austin, TX. American Society of Civil Engineers.

Sanders, B. F., (2007). Evaluation of on-line DEMs for flood inundation modeling. Adv Water Resour., 30(8): 1831–1843 (13 pages).

Santos, P.P.; Tavares, A.O., (2012). Hydraulic modelling of the flood prone area in a basin with a historical report of urban inundation: The Arunca River case (Central Portugal), in: Advances in safety, reliability and risk management. Taylor & Francis Group, London.

Scharffenberg, W.; Fleming, M.J., (2010). Hydrologic Modeling System (HEC-HMS) user's manual. Washington, DC: US Army Corps of Engineers.

Schumann G.; Matgen P.; Cutler M.E.J; Black A.; Hoffmann L.; Pfister, L., (2008). Comparison of remotely sensed water stages from LiDAR, topographic contours and SRTM. ISPRS J. Photogramm. Remote Sens., 63(3): 283-296 (14 pages).

Senate Economic Planning Office, (2013). Natural disaster at a glance.

Smith, M.J., (2010). Digital elevation models for research: UK datasets, copyright and derived products. Geol. Soc., Lond., Special Publ., 345(1): 129–133 (5 pages).

Ternate, J. R.; Celeste, M. I.; Pineda, E. F.; Tan, F. J.; Uy, F. A. A., (2017). Floodplain Modeling of Malaking-Ilog River in Southern Luzon, Philippines Using LiDAR Digital Elevation Model for the Design of Water-Related Structures. IOP Conference Series: Materials Science and Engineering, 216.

Tang, J.; Pilesjo, P., (2011). Estimating slope from raster data: a test of eight different algorithms in flat, undulating and steep terrain. JRBM, 146(4): 143-154 (12 pages).

Tom, P., (2018). Why do physical factors cause flooding? (AS-level standard).

UPD-TCAGP, (2013). Project 3: Modeling of flash flood events using integrated GIS and hydrological simulations. University of the Philippines–Diliman.

UPLB, (2017). Climate-responsive integrated master plan for Mindanao river basin. Executive summary. College of forestry and natural resources. Department of Environment and Natural Resources river basin control office. University of the Philippines – Los Baños.

USGS, (2008). Use of Light Detection and Ranging (LiDAR) to obtain high-resolution elevation data for Sussex Country, Deleware. Fact Sheet 2008-3088. United State Geological Survey.

USACE, (2010). Hydrologic Modeling System HEC-HMS user's manual. United States Army Corps of Engineers.

Wedajo, G.K., (2017). LiDAR DEM Data for flood mapping and assessment; opportunities and challenges: A review. JoRSG 6 (4): 1-4 (**4 pages**).

Weepener, H.L.; Van Den Berg, H.M.; Metz, M.; Hamandawana, H., (2012). The development of a hydrologically improved Digital Elevation Model and derived products for South Africa based on the SRTM DEM. Water Research Commission (WRC) Report No. 1908/1/11.

Werner, M. G. F., (2001). Impact of grid size in GIS based flood extent mapping using 1-D flow model. Physics and chemistry of earth (B). 26: 517–522 (**6 pages**).

Zhang, H.L.; Wang Y.J.; Wang, Y.Q.; Li, D.X.; Wang, X.K., (2013). The effect of watershed scale on HEC-HMS calibrated parameters: a case study in the Clear Creek watershed in Iowa, USA. HESSD, 10: 965-998 (**34 pages**).

AUTHOR (S) BIOSKETCHES

Ogania, J.L., B.Sc., Science Research Specialist, Geo-SAFER Project, College of Forestry and Environmental Science, Central Mindanao University, Musuan, Bukidnon, Philippines.. Email: *jeniferogania@gmail.com*

Puno, G.R., Ph.D., Associate Professor and Project Leader, Geo-SAFER Project, College of Forestry and Environmental Science, Central Mindanao University, Musuan, Bukidnon, Philippines.. Email: *geopuno@yahoo.com*

Alivio, M.B.T., B.Sc., Science Research Specialist, Geo-SAFER Project, College of Forestry and Environmental Science, Central Mindanao University, Musuan, Bukidnon, Philippines.. Email: *mnaryb@gmail.com*

Taylaran, J.M.G., B.Sc., Science Research Specialist, Geo-SAFER Project, College of Forestry and Environmental Science, Central Mindanao University, Musuan, Bukidnon, Philippines. Email: *johnmarktaylaran@gmail.com*

COPYRIGHTS

Copyright for this article is retained by the author(s), with publication rights granted to the GJESM Journal. This is an open-access article distributed under the terms and conditions of the Creative Commons Attribution License (http://creativecommons.org/licenses/by/4.0/).

HOW TO CITE THIS ARTICLE

Ogania, J.L.; Puno, G.R.; Alivio, M.B.T.; Taylaran, J.M.G., (2019). Effect of digital elevation model's resolution in producing flood hazard maps. Global J. Environ. Sci. Manage., 5(1): 95-106.

DOI: 10.22034/gjesm.2019.01.08

url: https://www.gjesm.net/article_33038.html